Second TNA Users Meeting

3 June 2025 | RMI, Brussels, Belgium

Combination of high rate ionosonde measurements with COSMIC-2 radio occultation observations: first results and future developments.

Iurii Cherniak [1], David Altadill [2], *Irina Zakharenkova* [1],
Víctor de Paula [2], Víctor Navas-Portella [2]
Douglas Hunt [1], Antoni Segarra [2]

[1] COSMIC Program Office, UCAR, Boulder, USA
[2] Observatori de l'Ebre (OE), CSIC - Universitat Ramon Llull, Roquetes, Terragona, Spain

UCAR COMMUNITY PROGRAMS COSMIC

Probing of altitudinal distribution of ionospheric plasma density: radio observations

HF sounding radars - ionosondes:
- unbiased plasma density values up to F2 peak
- globally distributed network at low, high and mid latitudes
- continuous 24/7 observations, basic dataset for ionospheric climatology

Incoherent scatter radars:
- full profile up to 1000 km altitude
- several sites at low, high and mid latitudes
- limited time observational complains, limitations for global climatology

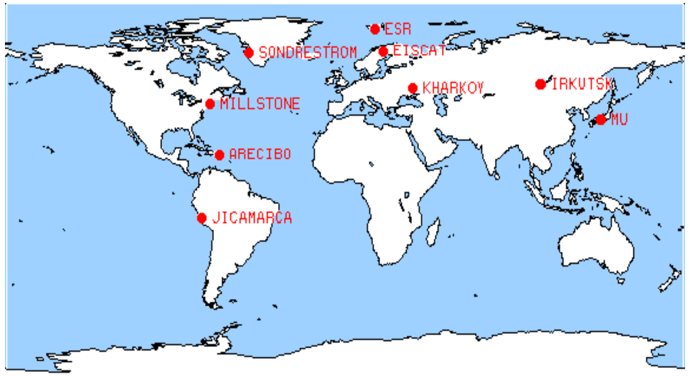

Radio occultation observations:
- full profile up to LEO altitude (500-700 km)
- global data coverage
- continuous observations suitable climatologic analysis

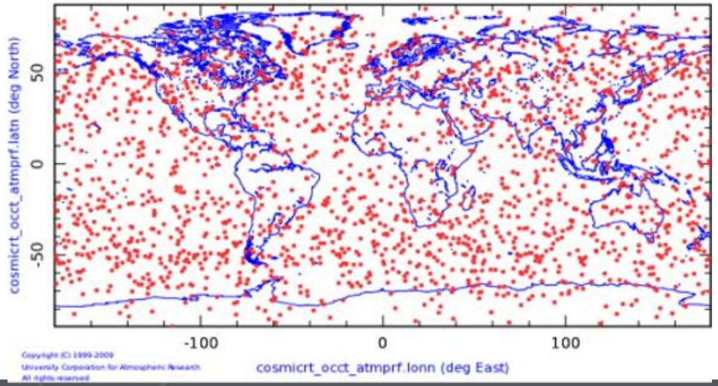

HF sounding radars (Ionosondes): Fundamentals

Developed in 1920s, ionosondes are still considered as the "benchmark" data source for unbiased measurements of electron density in the bottom side ionosphere, up to the ionospheric F2 peak height.

Served as "Ground true" for different instruments (manually scaled ionogramms)

Core dataset for climatological models

Ionospheric F2 layer peak parameters (NmF2 & hmF2) for profile – based models formulation

Continuous day-to day variability records for multiply sites globally distributed

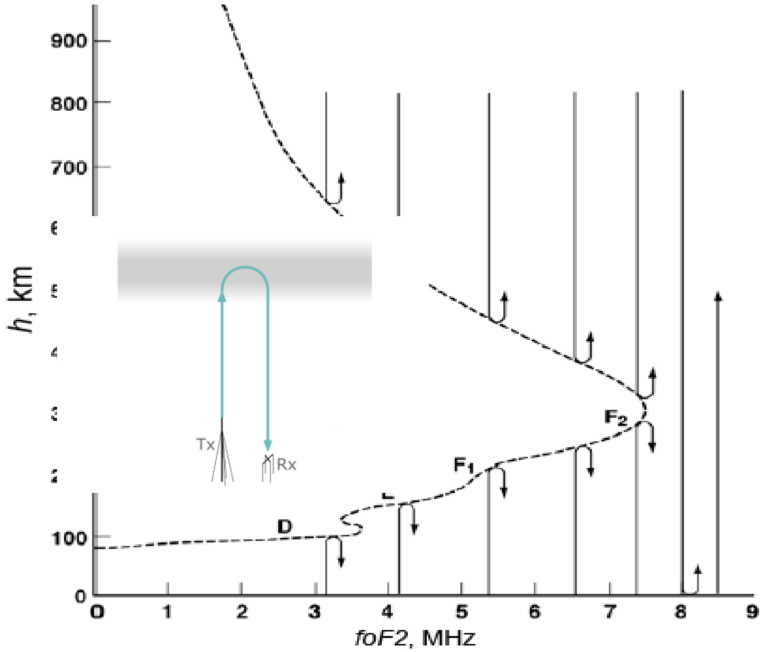

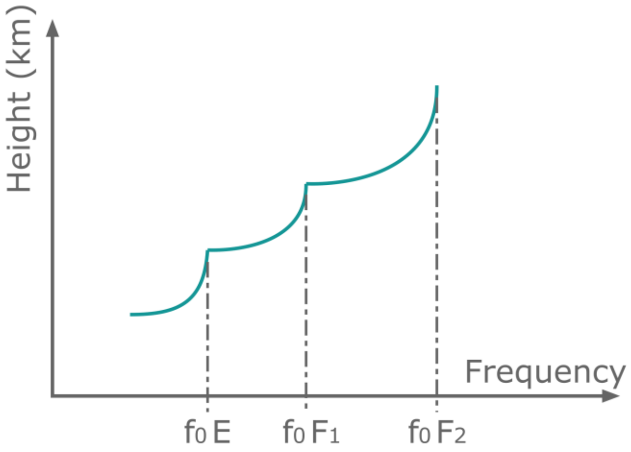

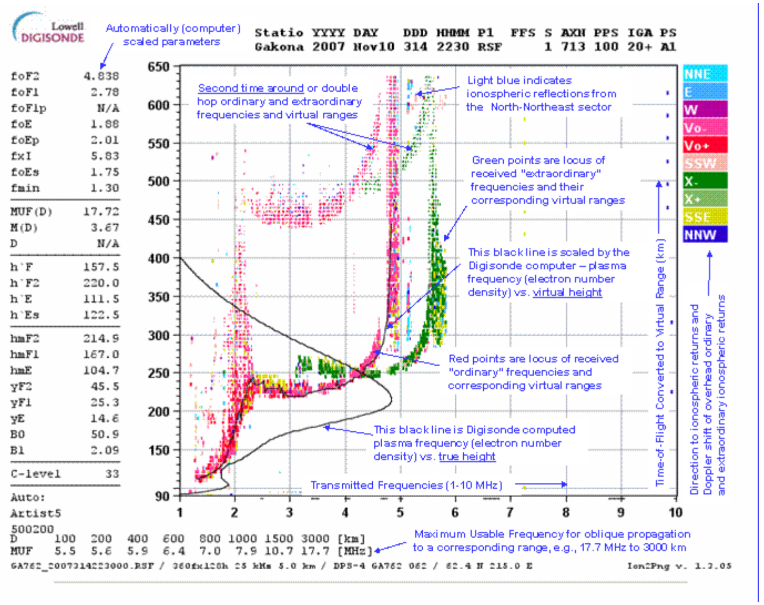

GNSS radio occultations from LEO for ionosphere probing: Fundamentals

- Inversion via onion-peeling approach to obtain electron density N(r)
- Assumption of spherical symmetry
- Assume straight-line propagation (the paths of L1 and L2 are the same)
- Assume that data are available for the back side (AB) link and that they traverse the same ionosphere that the front side (AC) link does.

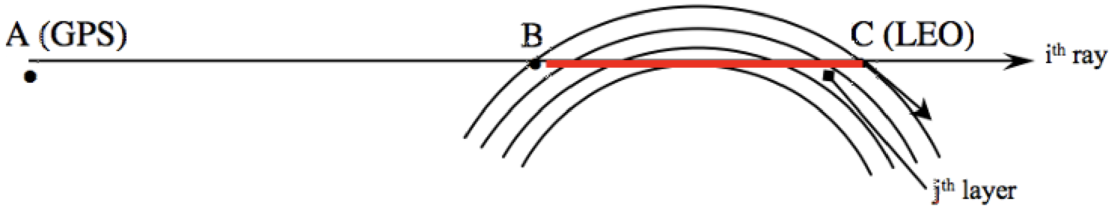

$$TEC \approx \frac{f_1^2 f_2^2 (L_1 - L_2)}{C(f_1^2 - f_2^2)}$$

where L_1,L_2 are phase measurements, m
and f_1,f_2 are GPS frequencies, Hz
and C = 40.3082

Adapted from Schreiner et all, 2006

Calibrated TEC below LEO:

$$\tilde{T}(r_0) = T_{BC}(r_0) = T_{AC}(r_0) - T_{AB}(r_0)$$

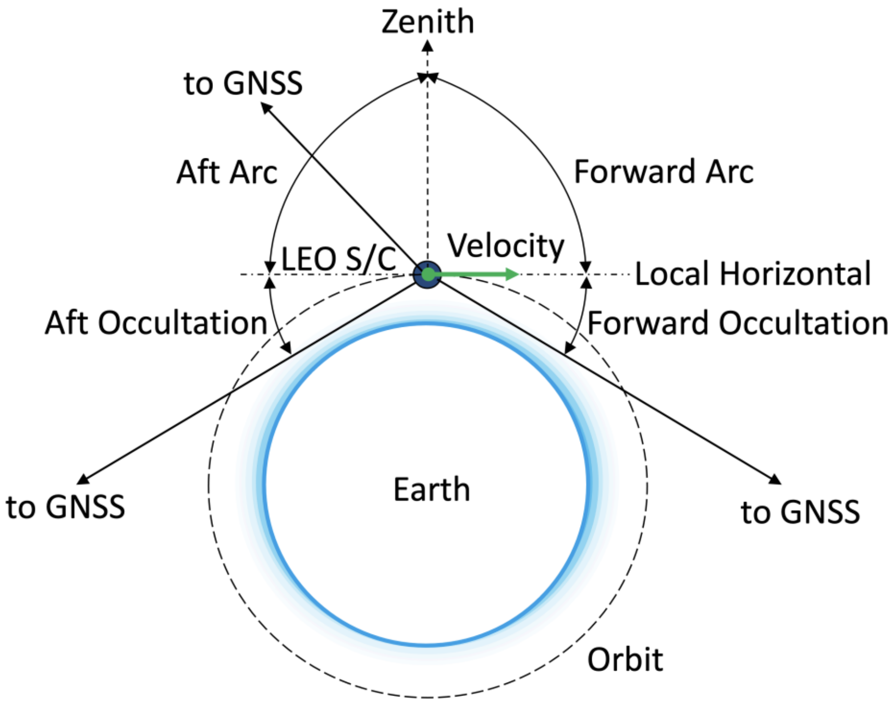

Assuming spherical symmetry and straight-line propagation:

$$\tilde{T}(p) = 2\int_p^{p_{top}} \frac{rN(r)}{\sqrt{r^2 - p^2}} dr\,.$$

The Abel transform

Where p is the distance from Earth's center to the tangent point of straight-line, and is the radius of the LEO.

$$p_{top} \equiv p_{leo}$$

Above equation inverted by Schreiner et al. (1999) to obtain

$$N(r) = -\frac{1}{\pi}\int_r^{r_{LEO}} \frac{d\tilde{T}/dp}{\sqrt{p^2 - r^2}} dp\,.$$

GNSS radio occultations from LEO for ionosphere probing: COSMIC-2 missions

6 satellites

Orbit inclination:
- 24°

Orbit Altitude:
- 540–550 km

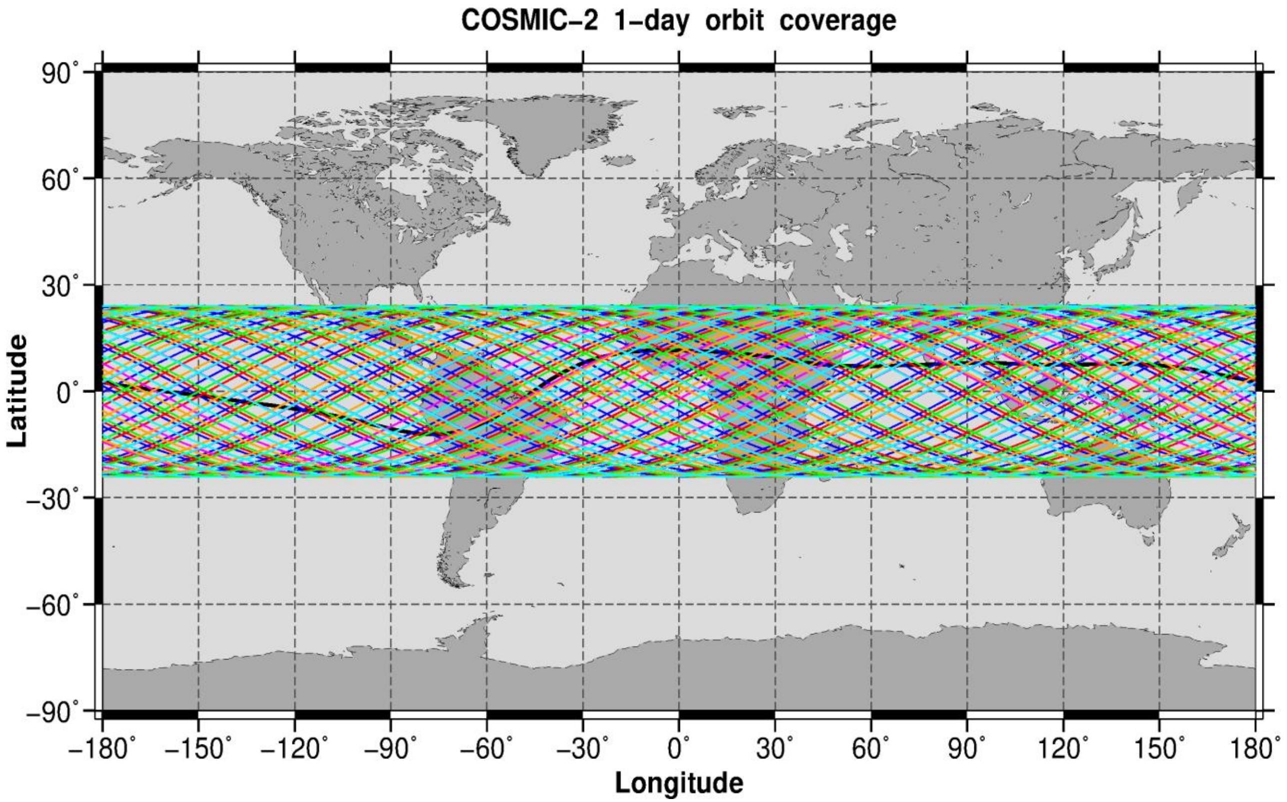

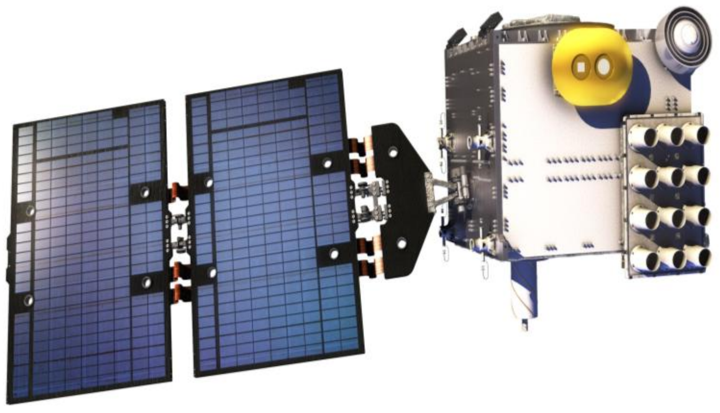

COSMIC-2 RO payload

TGRS (Tri-GNSS Radio Occultation Receiver System) developed by JPL

RO with GPS and GLONASS signals

- ✓ Slant TEC above and below an orbit
- ✓ **RO electron density profiles**
- ✓ S4 scintillation
- ✓ Plasma irregularities geolocations

GNSS radio occultations from LEO for ionosphere probing: COSMIC-2 missions

C2 Ionospheric Electron Density Profiles Level 2 data product

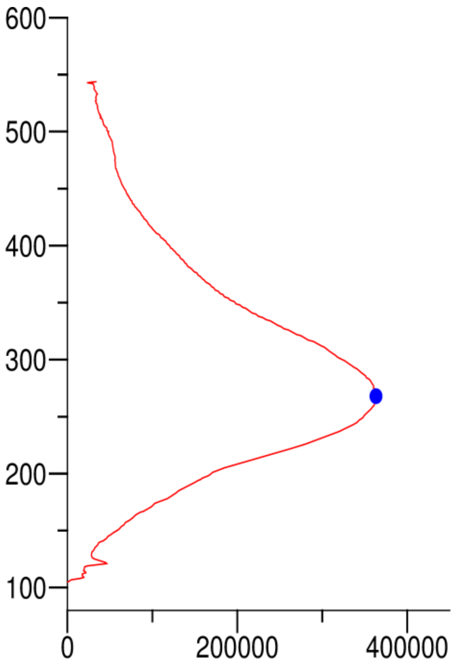

~ 5000 EDPs per day

~ 200 profiles per 1 hr

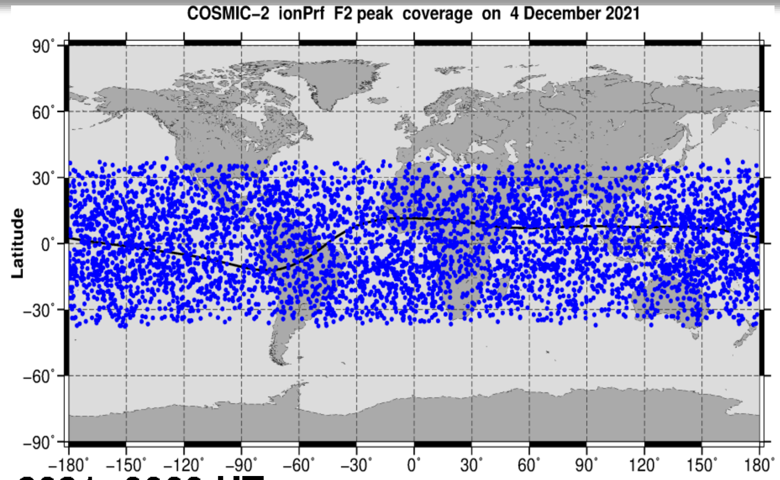

04 Dec 2021 0000 UT

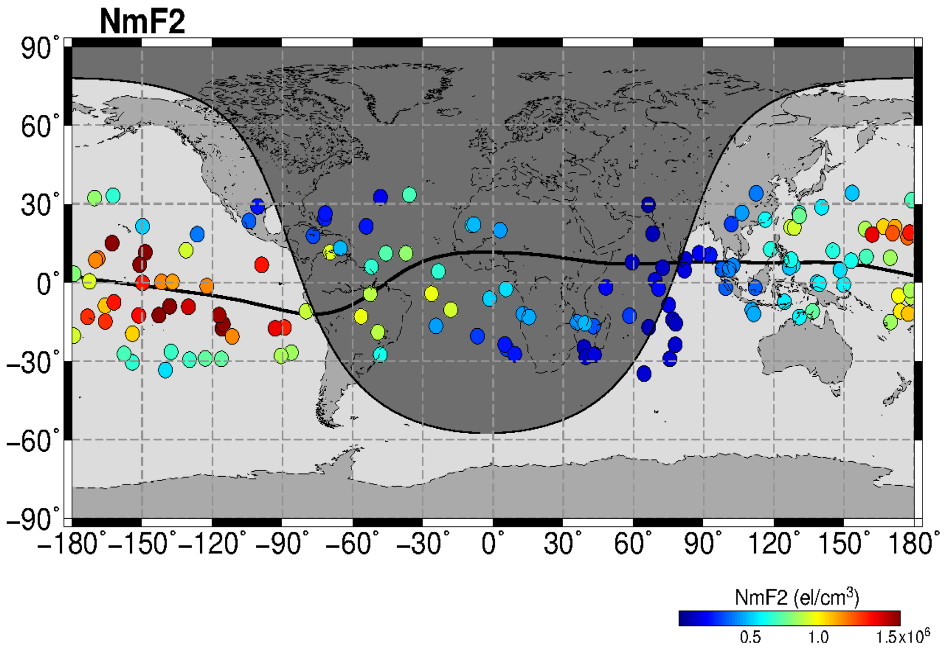

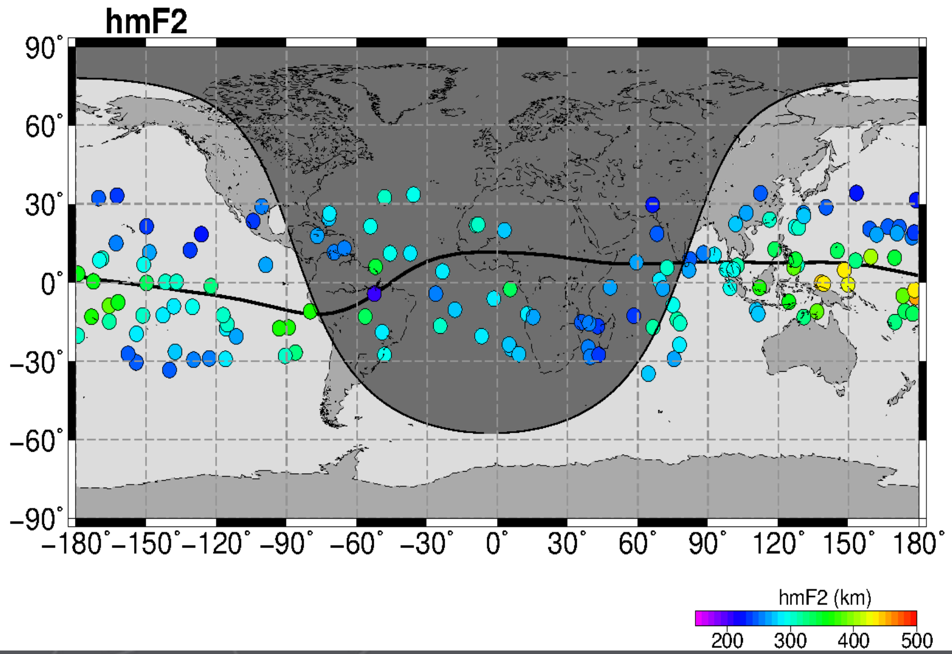

Available on COSMIC Data Analysis and Archive Center (CDAAC)

GNSS radio occultations from LEO for ionosphere probing: COSMIC-2 EDPs product validation

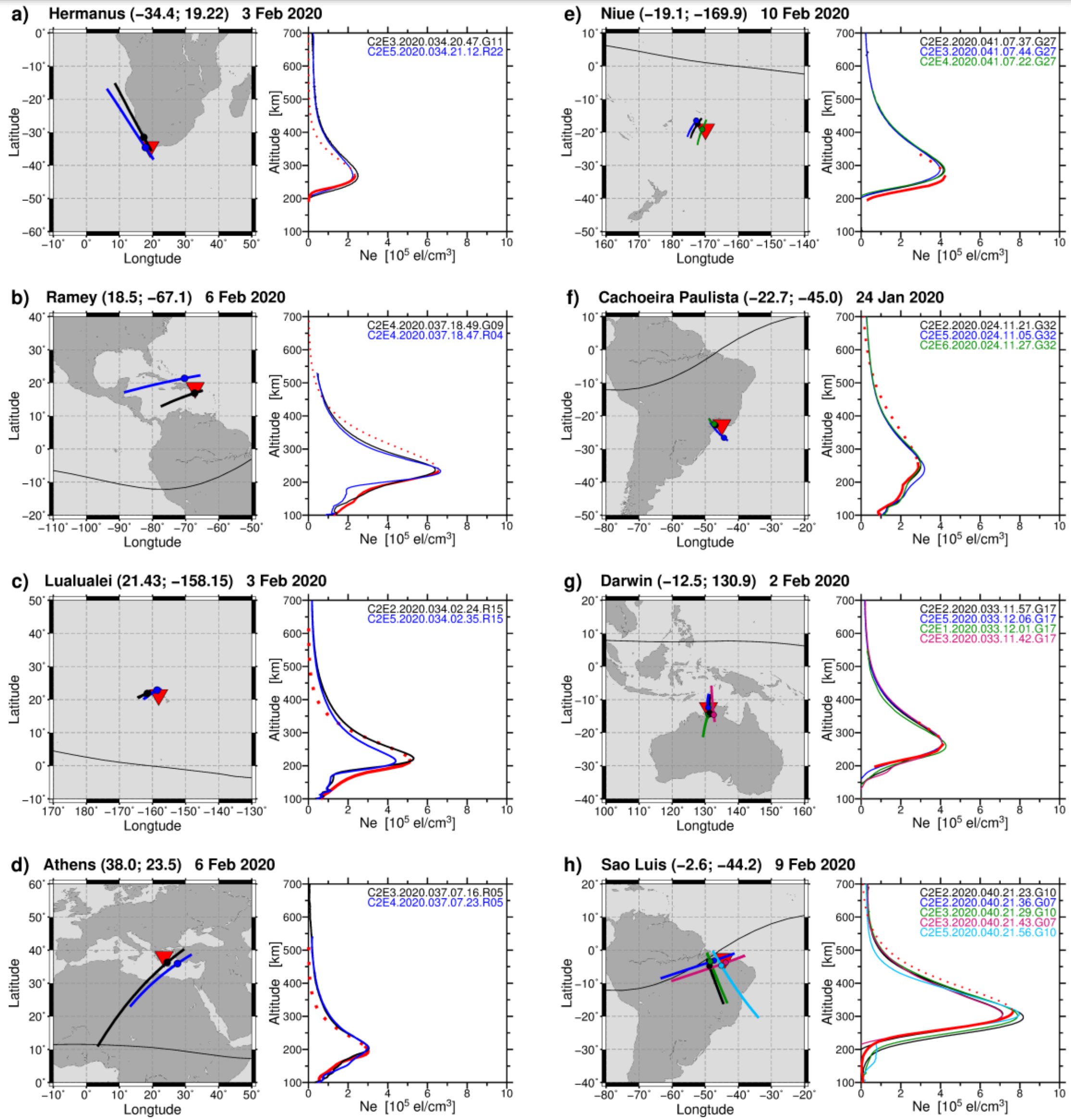

Performance and accuracy of Electron Density Profiles Level 2 data product were evaluated by ionosonde observations.

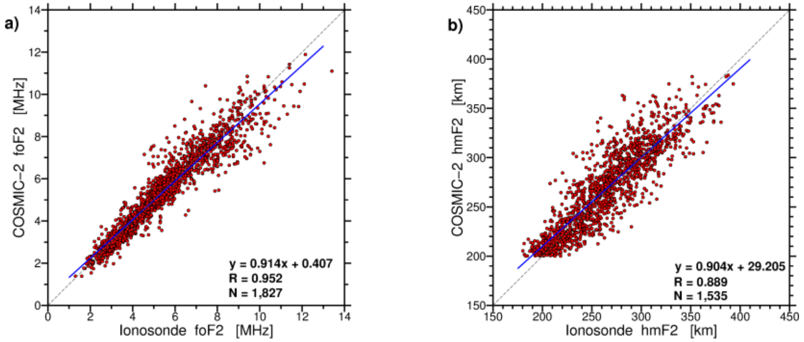

The scatter plots of the COSMIC-2 RO-based foF2 and hmF2 values against the corresponding ionosonde-derived ones.

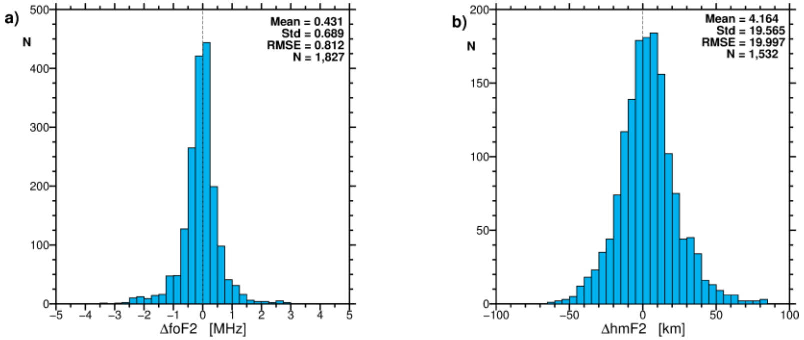

Histograms of the F2 peak parameters residuals ΔfoF2 (ΔfoF2 = $foF2_{RO}$ – $foF2_{ionosonde}$) and ΔhmF2 (ΔhmF2 = $hmF2_{RO}$ – $hmF2_{ionosonde}$) between collocated COSMIC-2 and ionosonde measurements

More details in Cherniak et al, JSWSC, 2021

Ionosonde's high-rate campaigns

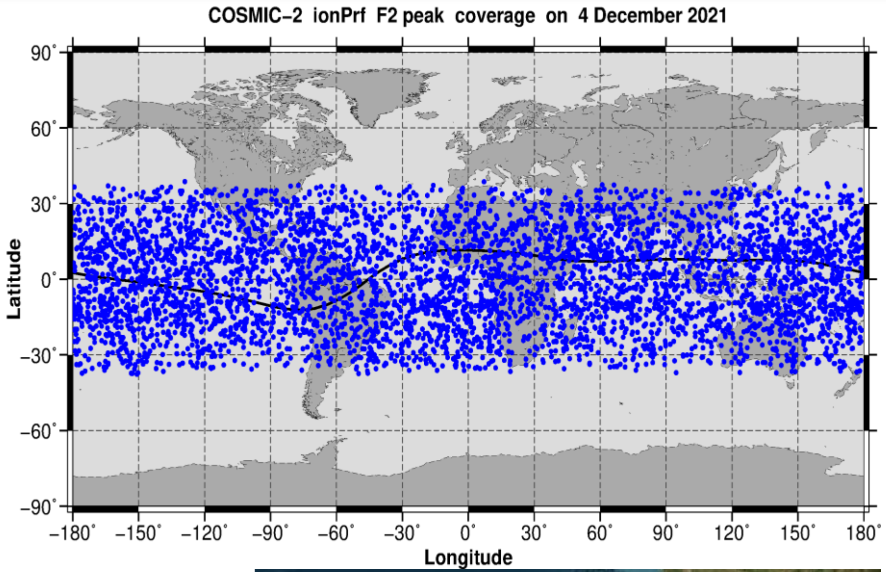

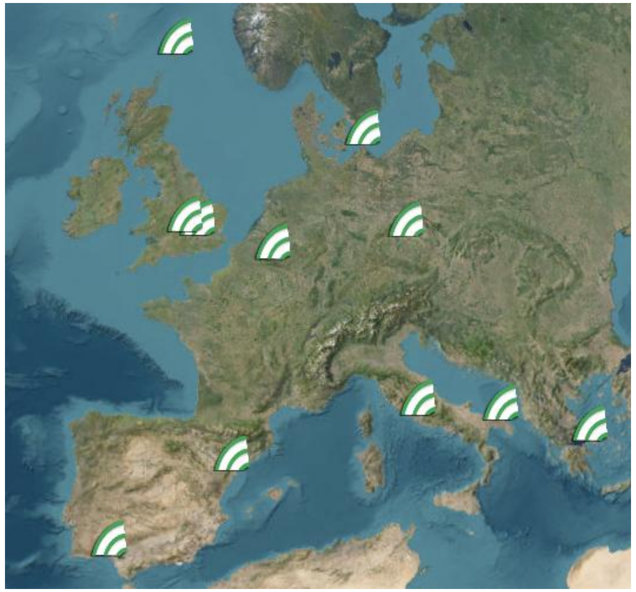

This study is inspired by the Ebre ionosonde's high-rate campaigns.

Two high rate datasets with 1-minute resolution ionograms are collected for to the October 2022 and March 2024. For the October 2022 high rate ionogtams also avaliable for El Arenosillo ionosonde

Both of time periods was close to the equinoxes, characterized by the quiet geomagnetic conditions (Kp=1-2) on bacground of low (!75 SFU) and high solar activity levels (~170 SFU).

COSMIC-2 RO vs ionosondes colocation

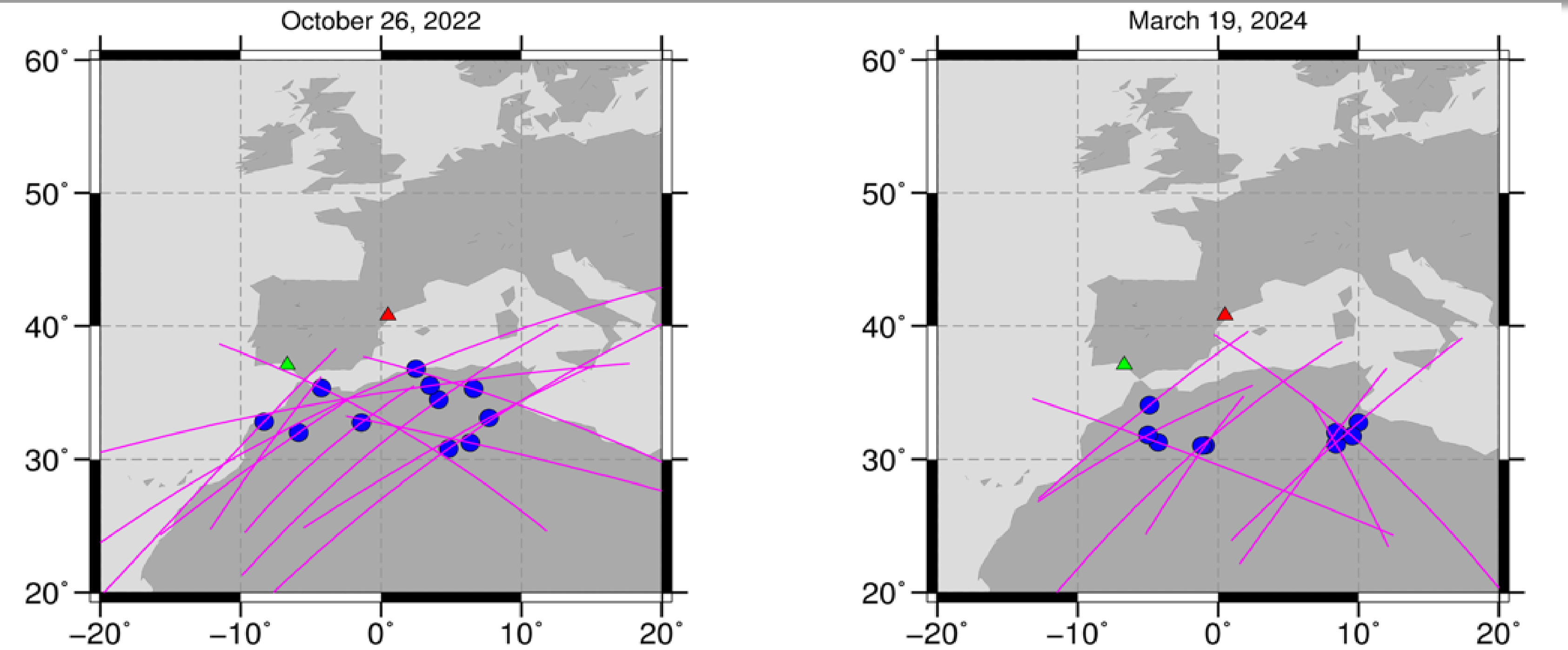

COSMIC-2 RO observations with EDP tangent point projections (pink lines) for 26 October 2022 and 19 March 2024.

The blue dots corresponded to the F2 layer peak location derived from COSMIC-2 RO profiles. Red and green triangles pinpoint the Ebre and El Arenosillo ionosondes locations, respectively.

Colocation criteria for the GNSS RO vs ionosonde measurements are based on the spatial correlation factor of ionospheric plasma density variability. For the quiet-time midlatitude ionosphere, the correlation distance (correlation coefficient r > 0.70) can be considered as approximately 1,500–3,000 km in an east-west direction and 1,000–1,800 km in a north-south direction.

Important advantage of high-rate ionosonde compains is that we can obtain more precise colocations in temporal domain.

The expert mode ionograms analysys

All high rate ionogtams for this study were processed manually in "expert mode" by the ionogram interpretation specialists of Ebre Observatory.
Such expert scaling of digital ionograms allows to get the precise virtual height - frequency inversion to the electron density profiles, as well as accurate estimates the major F2 peak parameters.

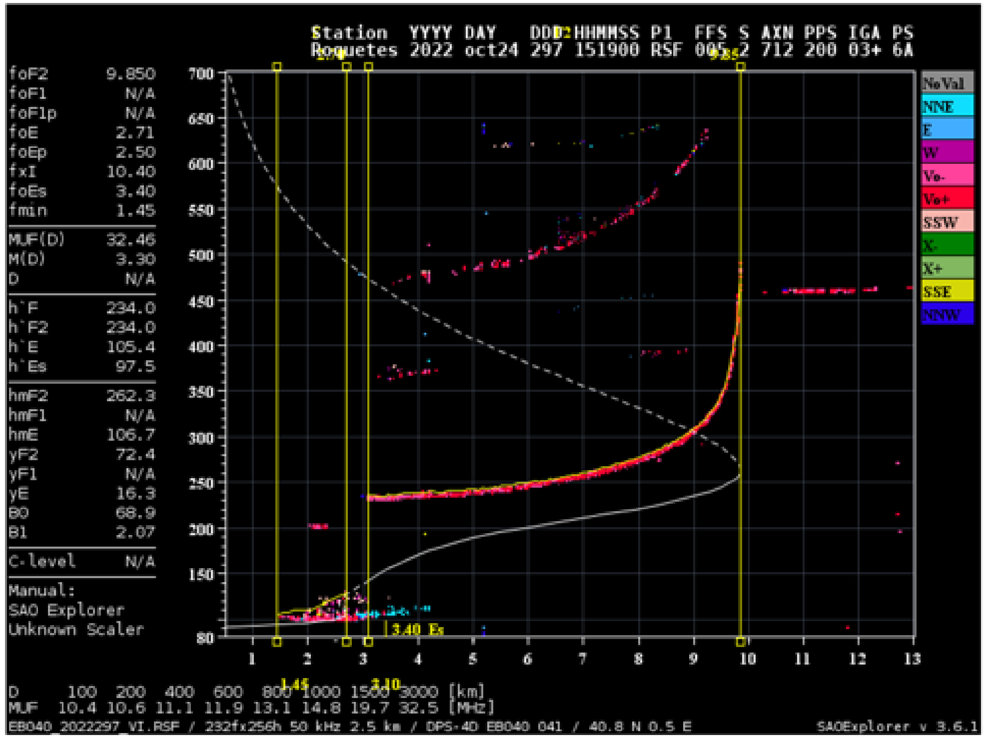

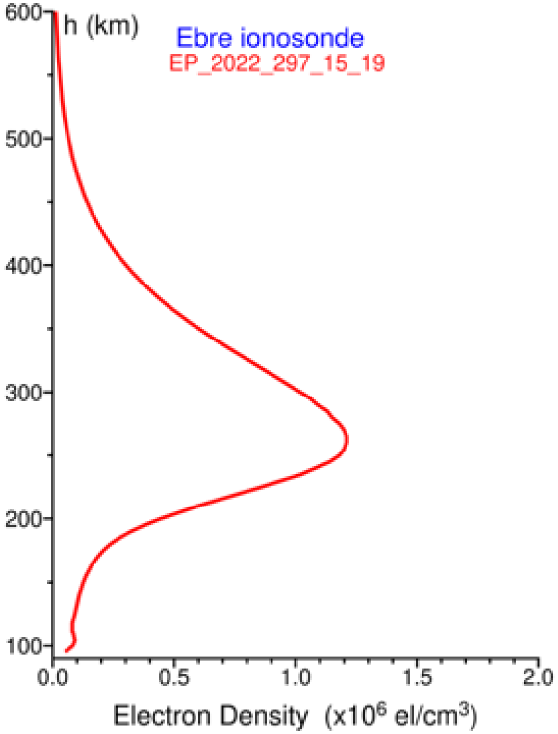

Example (from left to right) of the ground-based HF (ionosonde) sounding recording with results of the ionogram processing, and ionosonde-derived electron density profile Ne(h).

Remarks about LEO GNSS RO EDPs quality control

LEO GNSS RO EDPs are not exactly vertical, but 3-dimentional

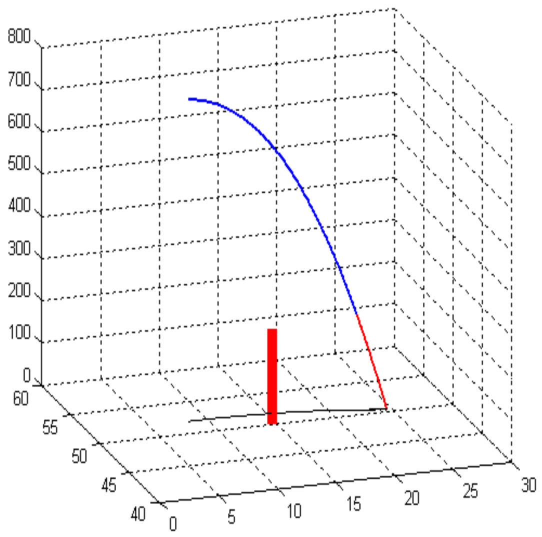

No quality control flags curentely implemented to the COSMIC EDPs

The data outliers are not filtered out from the EDPs product

The EDPs quality acessement should be done on the user side depending on applications.

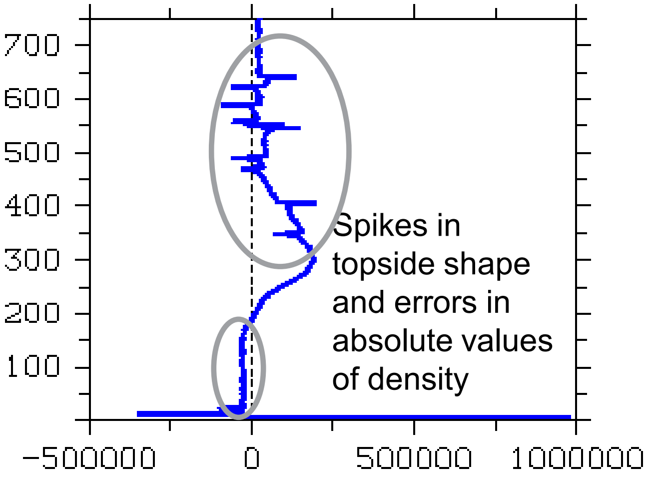

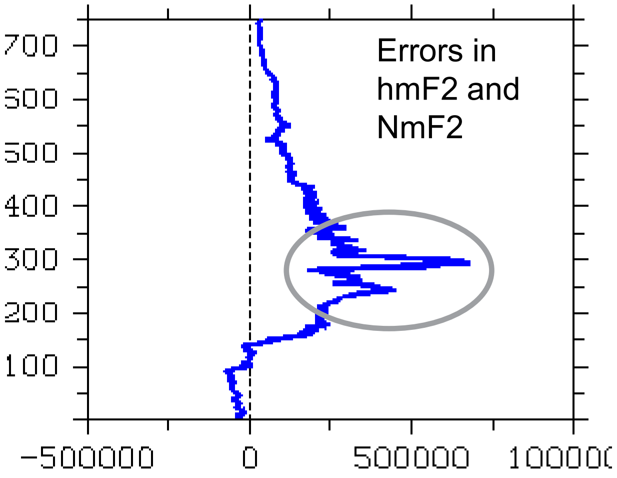

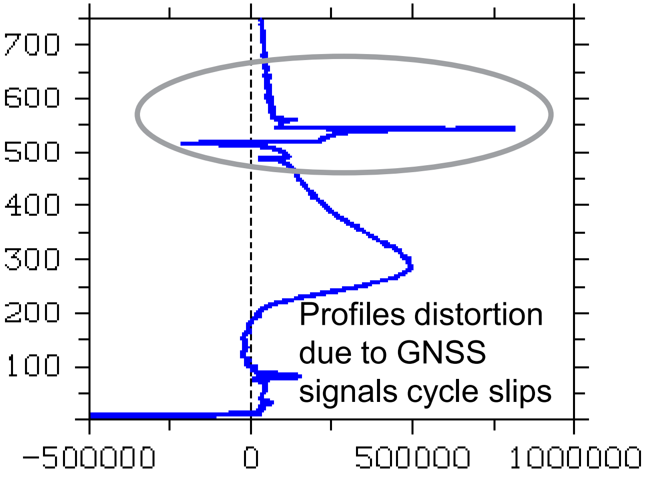

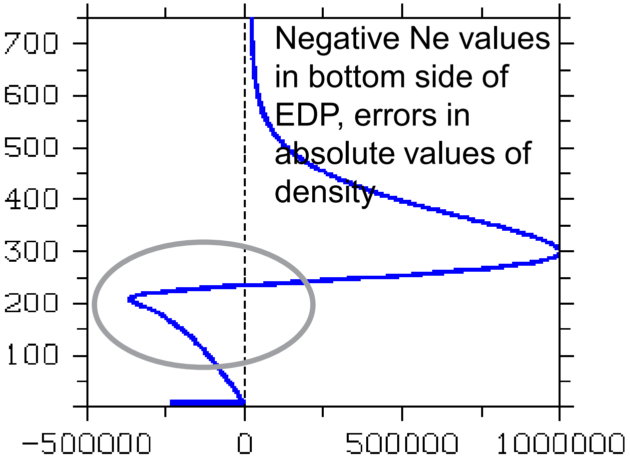

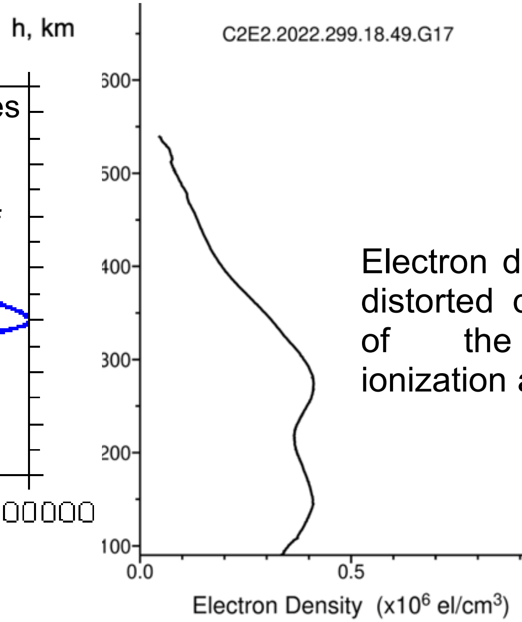

Electron density profiles distorted due to impact of the equatorial ionization anomaly

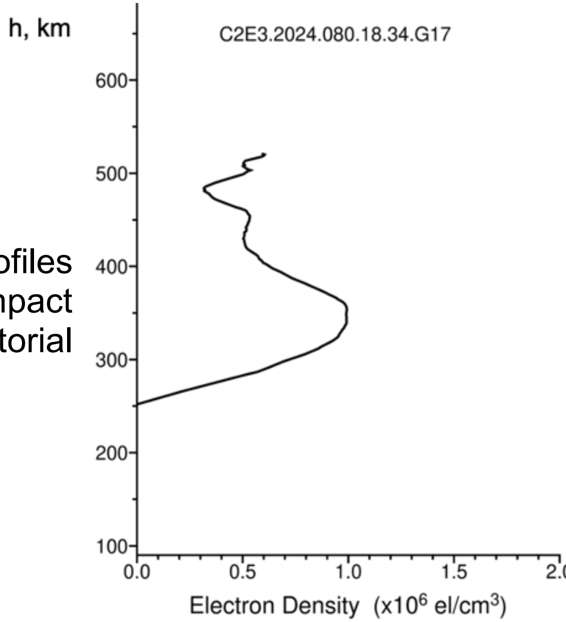

COSMIC-2 RO vs ionosondes EDPs. Ebre Observatory

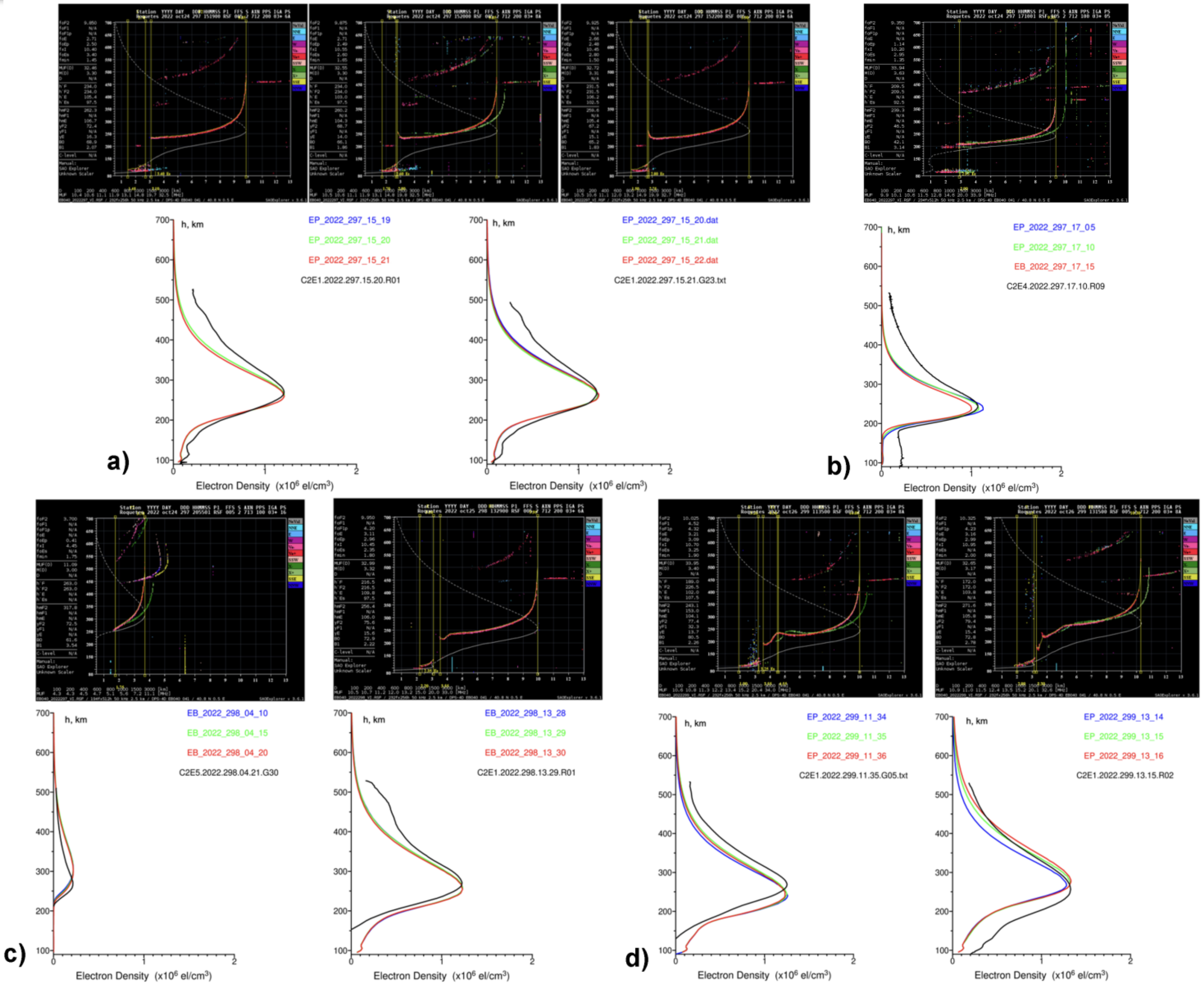

Representative examples of EDP colocation events between COSMIC-2 RO and Ebre ionosonde combining ionogram recording and EDP comparisons for the October 2022 high-rate sounding campaign.

The black line displays the COSMIC-2 RO EDP; the blue, green and red lines show the time sequence of several ionosonde-derived EDPs.

File names like "C2E1.2022.297.15.20.R01" mean COSMIC-2 satellite C2E1, year 2022, DOY (day-of-year) 297, time 15:20 UT, "R01"– tracking GLONASS satellite PRN 01. Ionosonde file names in plot captions shared a similar structure.

COSMIC-2 RO vs ionosondes EDPs. Ebre Observatory

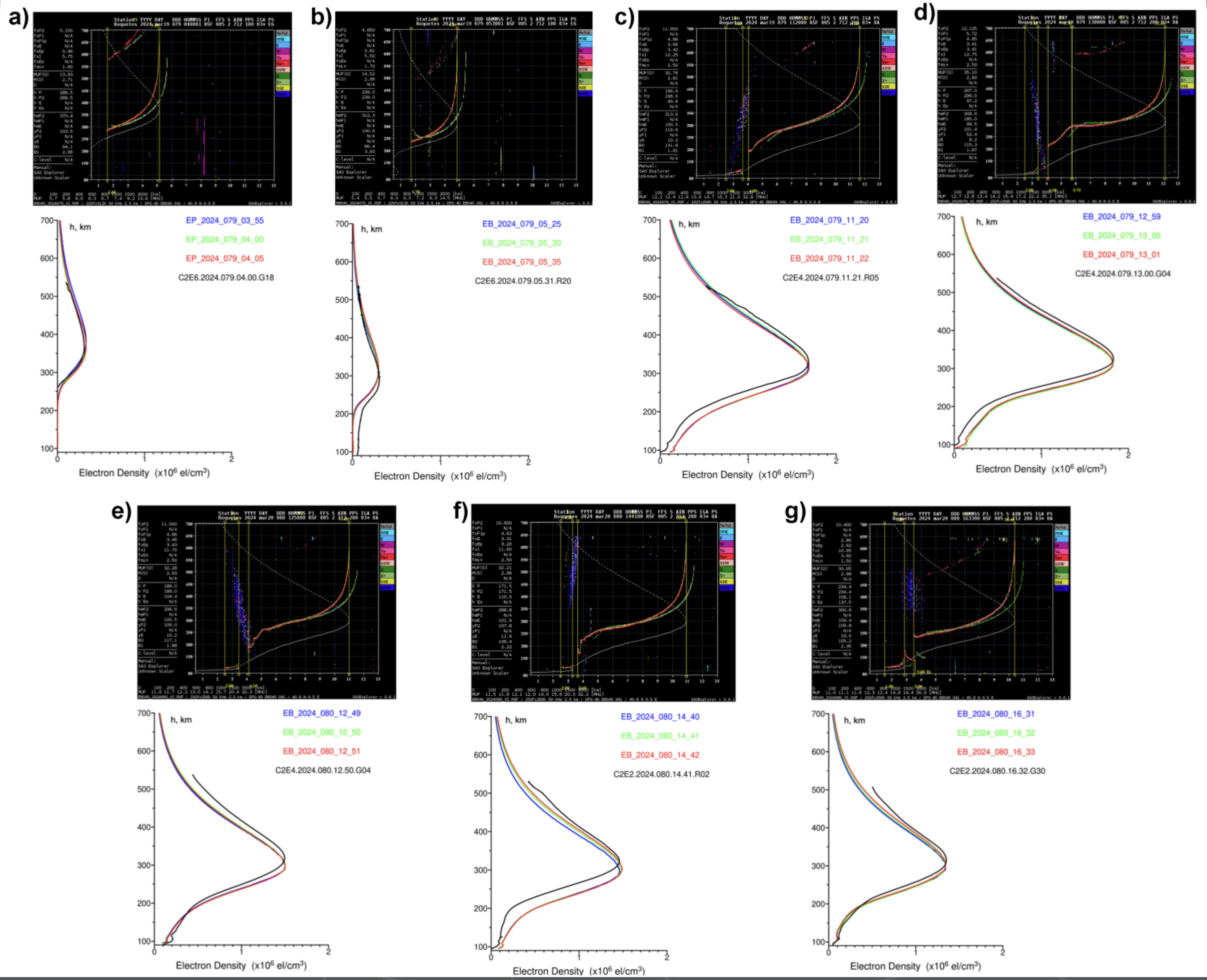

Representative examples of EDP colocation events between COSMIC-2 RO and Ebre ionosonde combining ionogram recording and EDP comparisons for the March 2024 high-rate sounding campaign.

The black line displays the COSMIC-2 RO EDP; the blue, green and red lines show the time sequence of several ionosonde-derived EDPs.

COSMIC-2 RO vs ionosondes EDPs. El Arenosillo Observatory

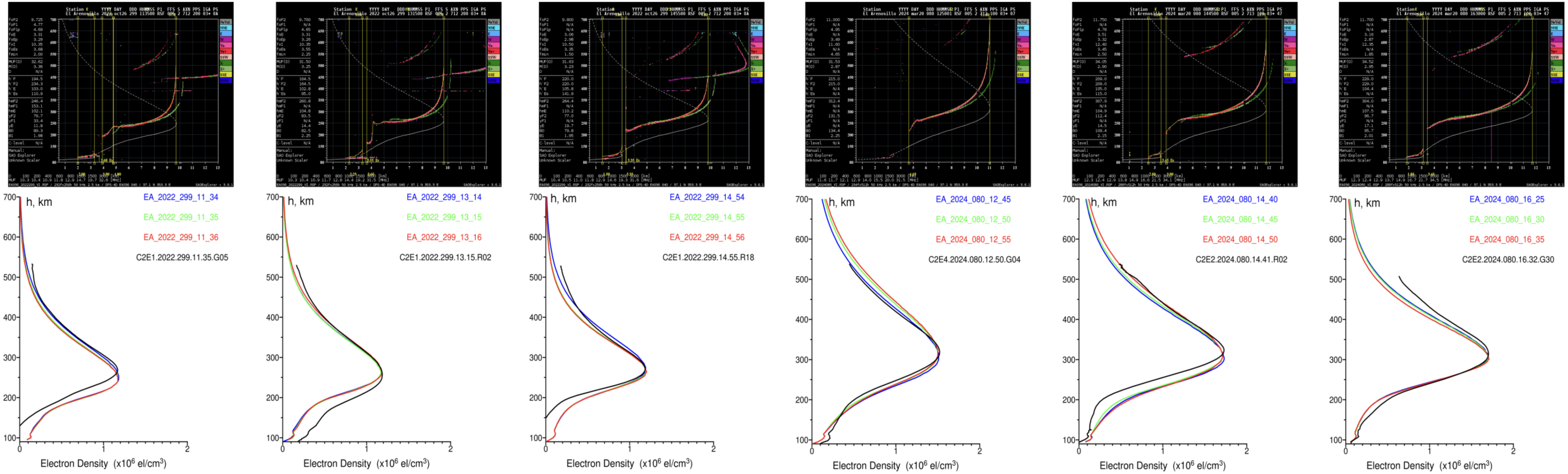

Representative examples of EDP colocation events between COSMIC-2 RO and El Arenosillo ionosonde combining ionogram recording and EDP comparisons for the October 2022 (left) and the March 2024 (right) high-rate sounding campaign.

Combined ionospheric EDPs as a **new data source for validation of climatological models of ionosphere**

IRI

Model Developers: Dieter Bilitza, NASA, International IRI Working Group

Model Input
Solar indices (F10.7 index, sunspot number),
Ionospheric index (IG)
magnetic indices (Ap and Kp)
URSI/CCIR maps of model coefficients (foF2)

Model Output
Height range: 80 – 2,000 km
Electron density& temperature
Ion density
Ion composition
Ionospheric total electron content (TEC)

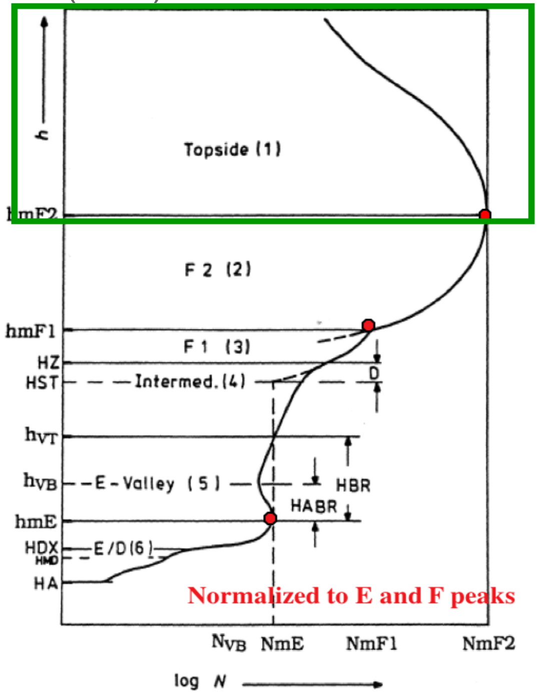

IRI is a ISO standard

Global models for foF2/NmF2 foF1/NmF1, foE/NmE, hmF2, hmF1 , hmE

NeQuick

Model Developers: S. Radicella, B. Nava, ICTP

Model Input
Solar indices (F10.7 index, sunspot number),
ITU-R (former CCIR) coefficients

Model Output
Electron density
Height range: 80 – 20,000 km
Ionospheric total electron content (TEC): vTEC and sTEC

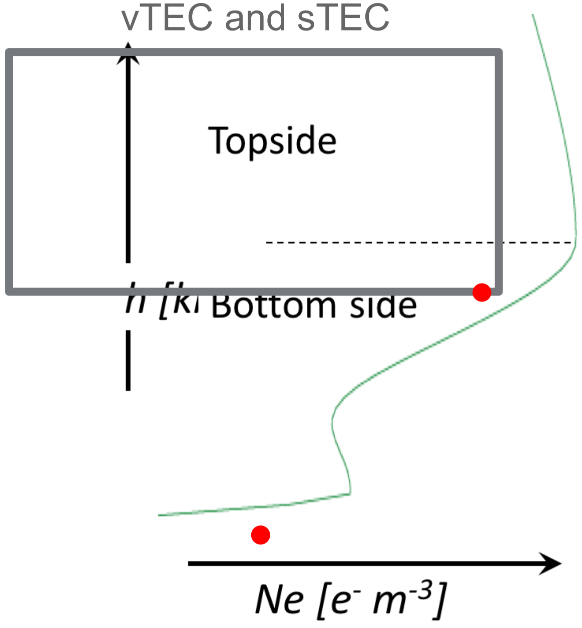

Profiler model - 6 semi-Epstein layers with modeled thickness parameters and is based on anchor points defined by foE, foF1, foF2 and M(3000)F2 values.

$$N_{Epstein}(h; hmax, Nmax, B) = \frac{4Nmax}{\left(1+\exp\left(\frac{h-hmax}{B}\right)\right)^2}\exp\left(\frac{h-hmax}{B}\right)$$

Combined ionospheric EDPs as a **new data source for validation of climatological models of ionosphere**

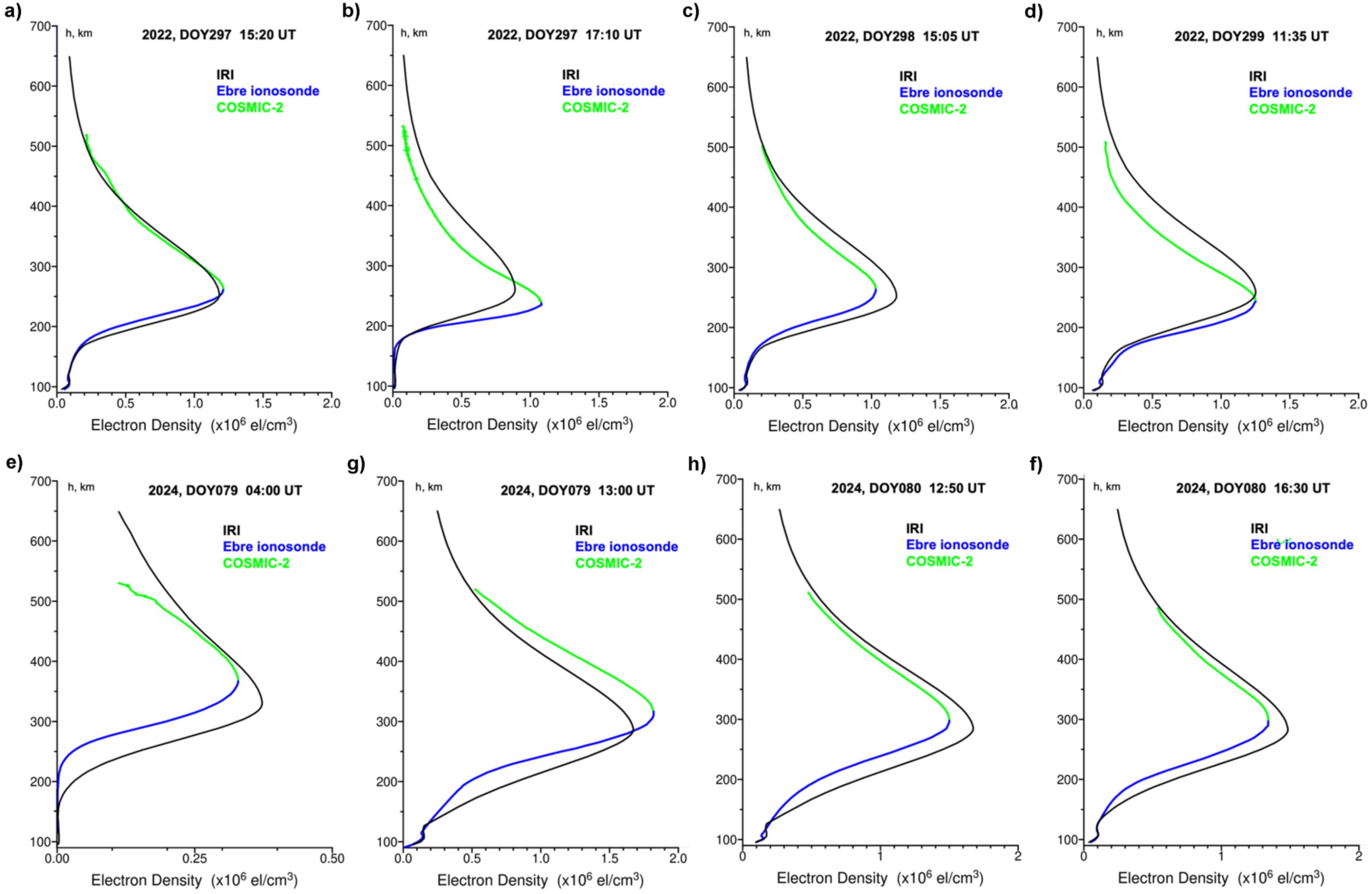

Comparison of the electron density profiles derived from the IRI-2020 (black line) and the reference profiles combined from ionosonde (blue) and COSMIC-2 RO (green) measurement.

The obtained results demonstrate clear differences in the EDPs shape and peak values (up to 20% in density) in the model simulation outputs between the standard IRI and the corrected version with the real F2 layer peak values.

Combined ionospheric EDPs as a **new data source for validation of climatological models of ionosphere**

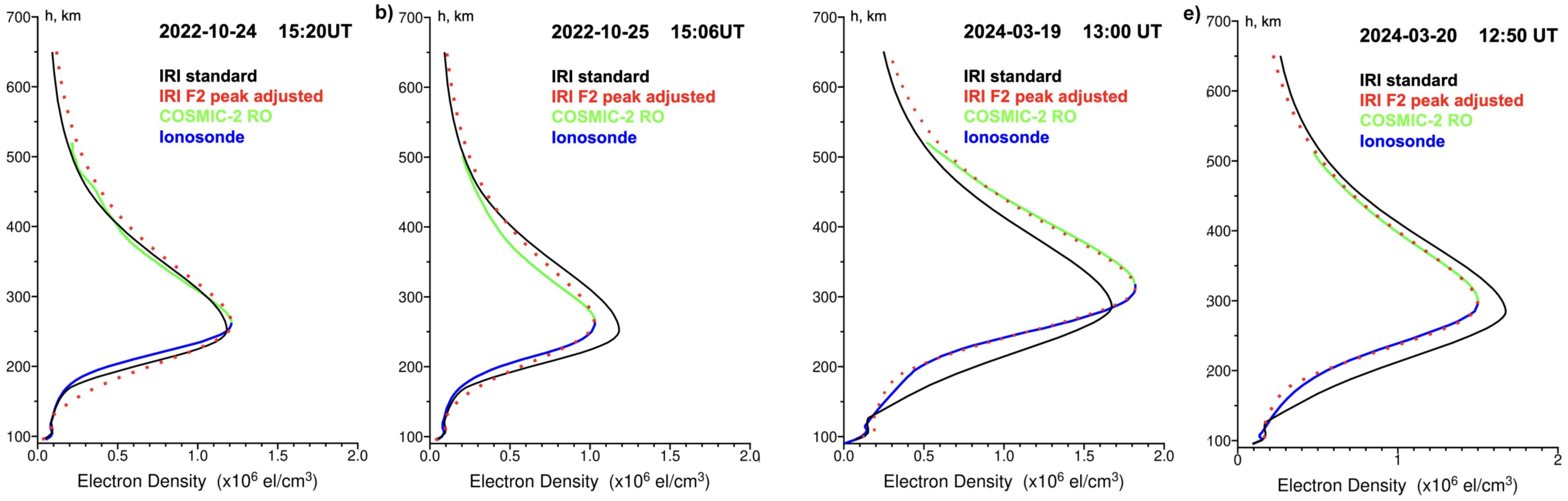

Comparison of the IRI-2020 adjusted EDPs (red dots) with reference combined EDPs (blue-green line). The standard IRI output is shown as a black line.

Future developments:
Exploring advantages of GEO GPS RO and ionosondes combination

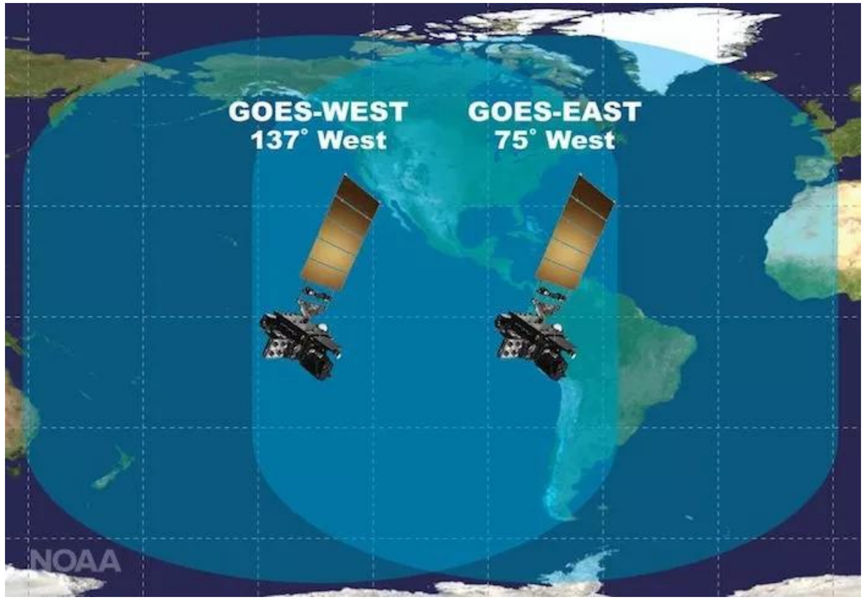

Due to GPS antenna beam width limitations, all GPS visible from GOES are behind the Earth

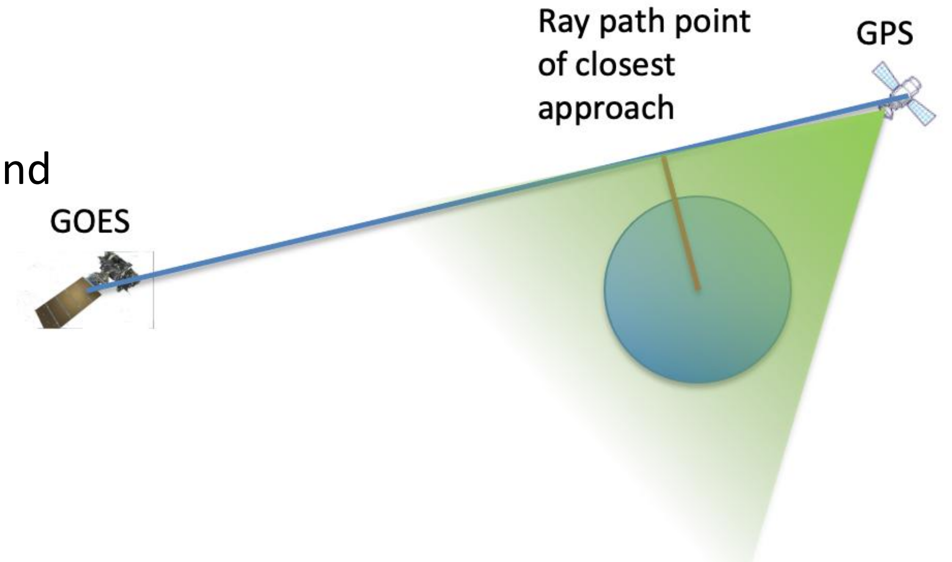

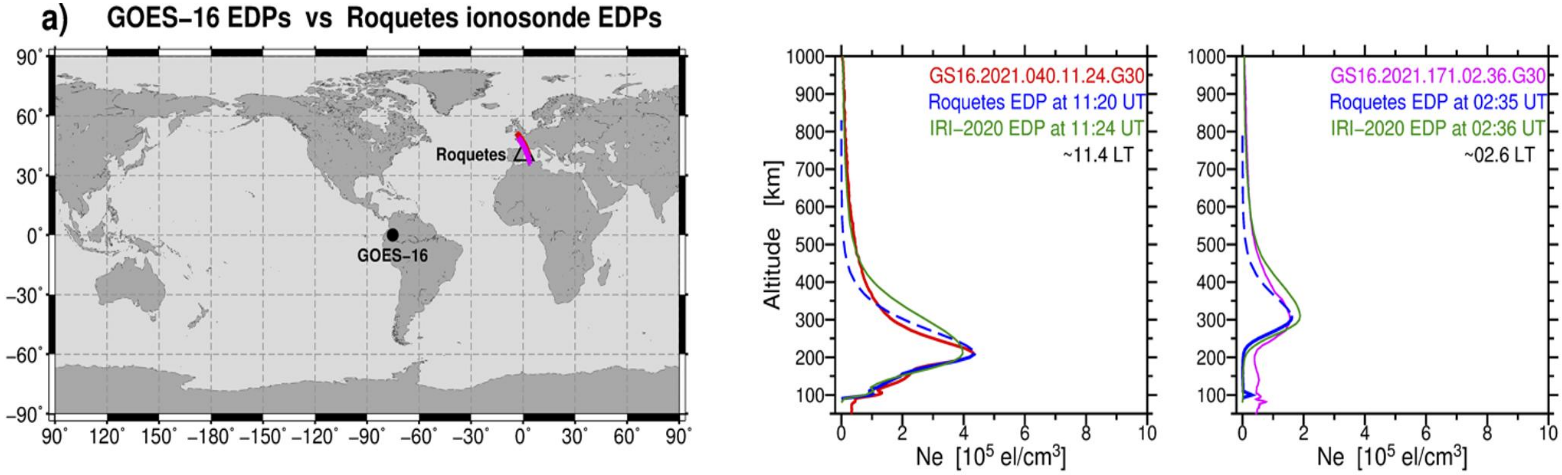

Geostationary Operational Environmental Satellite (GOES) used by NOAA and NASA for real-time Earth monitoring and weather prediction

GOES system are equatorial satellites with orbit altitude is ~35800 km.

- **GOES-16,** GOES-East (75.2°W)
- **GOES-17,** GOES-West (137.2°W)
- Satellites are equipped by single frequency GPS receiver for orbit tracking

Future developments:
Joint high rate ionosonde measurements and with COSMIC-2 radio occultation for ionospheric clymatology

Discussion possibilities of regular **high rate ionosonde compai** equinox and solstices

Summary

- During realization of this project, the participants from the TNA Node of Ebro Observatory and UCAR COSMIC worked together as a research team for analysis and exploitation of ionosonde and GNSS RO data.

- By analyzing high-sampling-rate observations from Ebre and El Arenosillo ionosonde stations with collocated COSMIC-2 RO measurements, we demonstrated possibilities to develop a new experimental data source for specification of ionosphere plasma density vertical distribution - combined ionospheric EDPs based solely on real high-quality observations from both the bottomside and topside parts of the ionosphere.

- Such combined EDPs can serve as analogy of incoherent scatter radar derived "full profiles", providing a reference for altitudinal distribution of ionospheric plasma density.

- These reference profiles offer a valuable data source for validating and further improvement of the empirical and first principal and assimilative ionospheric models.

-

Acknowledgements

We acknowledge COSMIC CDAAC for providing RO electron density profiles from COSMIC-2 mission (UCAR COSMIC Program, https://doi.org/10.5065/t353-c093)

Raw ionograms from the Ebre and El Arenosillo digisondes are available through the GIRO database (http://giro.uml.edu/)

This research was funded by the PITHIA-NRF project. The PITHIA-NRF project has received funding from European Union's Horizon 2020 research and innovation programme under grant agreement No 101007599.

This research was partially funded by the National Science Foundation (Grant 2054356) and National Aeronautics and Space Administration (Grants C22K0658 and 80NSSC20K1733).

Thank you for your attention!